Brief Definitive Report

Evidence for a Role of Mast Cells in the Evolution to Congestive Heart Failure

Masatake Hara,[1] Koh Ono,[1] Myung-Woo Hwang,[1] Atsushi Iwasaki,[1] Masaharu Okada,[1] Kazuki Nakatani,[2] Shigetake Sasayama,[1] and Akira Matsumori[1]

[1]*Department of Cardiovascular Medicine, Kyoto University Graduate School of Medicine, Kyoto 606-8397, Japan*
[2]*Second Department of Anatomy, Osaka City University Medical School, Osaka 545-8585, Japan*

Abstract

Mast cells are believed to be involved in the pathophysiology of heart failure, but their precise role in the process is unknown. This study examined the role of mast cells in the progression of heart failure, using mast cell-deficient (WBB6F1-W/W^v) mice and their congenic controls (wild-type [WT] mice). Systolic pressure overload was produced by banding of the abdominal aorta, and cardiac function was monitored over 15 wk. At 4 wk after aortic constriction, cardiac hypertrophy with preserved left ventricular performance (compensated hypertrophy) was observed in both W/W^v and WT mice. Thereafter, left ventricular performance gradually decreased in WT mice, and pulmonary congestion became apparent at 15 wk (decompensated hypertrophy). In contrast, decompensation of cardiac function did not occur in W/W^v mice; left ventricular performance was preserved throughout, and pulmonary congestion was not observed. Perivascular fibrosis and upregulation of mast cell chymase were all less apparent in W/W^v mice. Treatment with tranilast, a mast cell–stabilizing agent, also prevented the evolution from compensated hypertrophy to heart failure. These observations suggest that mast cells play a critical role in the progression of heart failure. Stabilization of mast cells may represent a new approach in the management of heart failure.

Key words: heart failure • mast cells • left ventricular hypertrophy • pressure overload • chymase

Introduction

When the heart is exposed to pressure overload, cardiac hypertrophy develops to preserve its function by normalizing chamber wall stress (1). If mechanical overload persists, the hypertrophied heart dilates and its contractile function decreases, resulting in congestive heart failure (1). The mechanism of transition from compensated hypertrophy to heart failure has not been clarified (2).

Mast cells are found in the human heart (3), and have been implicated in cardiovascular diseases (4, 5). They were increased in both hypertrophied (5) and failing hearts (6). However, their role in the pathophysiology of cardiac hypertrophy and failure is unclear. We have recently observed that mast cells cause apoptosis of cardiac myocytes and proliferation of nonmyocytes in vitro (7). As loss of cardiac myocytes and proliferation of nonmyocytes both result in cardiac dysfunction (1), we hypothesized that myocardial mast cells may be implicated in the progression of heart failure.

This study was performed to examine whether mast cells play a role in the evolution from compensated hypertrophy to heart failure in a murine model of systolic pressure overload, using W/c-kit mutant WBB6F1-W/W^v mice, in which mast cells are nearly absent, and tranilast, a mast cell–stabilizing agent.

Materials and Methods

All experiments were performed in 9-wk-old male mice, obtained from Shizuoka Agricultural Cooperation Association, and treated in accordance with local institutional guidelines at all stages of the experiments.

Experiment 1. Male W/W^v mice (n = 25), or their normal male littermates, WBB6F1-+/+ (wild-type [WT]) mice (n = 24), were exposed to 15 wk of pressure overload produced by banding of the abdominal aorta with minor modifications of a

Address correspondence to Akira Matsumori, Department of Cardiovascular Medicine, Kyoto University Graduate School of Medicine, 54 Kawaracho Shogoin, Sakyo-ku, Kyoto 606-8397, Japan. Phone: 81-75-751-3186; Fax: 81-75-751-6477; E-mail: amat@kuhp.kyoto-u.ac.jp

 J. Exp. Med. © The Rockefeller University Press • 0022-1007/2002/02/375/07 $5.00
Volume 195, Number 3, February 4, 2002 375–381
http://www.jem.org/cgi/content/full/195/3/375

method described previously (8). The mice were anesthetized by intraperitoneal injection of a mixture of ketamine, 100 mg/kg, and xylazine, 5 mg/kg. The abdominal aorta was banded at the suprarenal level with 5–0 silk suture material ligated around the vessel and a 26-gauge needle, following which the needle was withdrawn. In addition, 14 W/W^v mice and 11 WT mice underwent identical surgical procedures, except for banding of the abdominal aorta (sham-operated controls). At 4 wk after operation, 10 W/W^v mice and 10 WT mice were killed to examine the role of mast cells in compensated hypertrophy. Thereafter, the remainder of the mice were followed with serial echocardiography, and killed at 15 wk to examine the role of mast cells in congestive heart failure analyses.

Mast Cell Reconstitution of W/W^v Mice. Mast cell reconstitution of W/W^v mice was performed as described previously (9). Bone marrow cells from femurs of male WT mice were cultured for 3 wk in WEHI-3 conditioned medium. To generate W/W^v+MC mice, adoptive transfer of mast cells (>98% purity) into the hearts of W/W^v mice was achieved by intravenous injection of 5×10^6 mast cells, 2 d before aortic banding. The mice were killed 15 wk after mast cell reconstitution and aortic banding. The density of cardiac mast cells was confirmed by staining with toluidine blue.

Bone Marrow Reconstitution of W/W^v Mice. The bone marrow reconstitution method has been described previously (10). Briefly, WT mice were killed by cervical dislocation, and the bone marrow was flushed with RPMI 1640 culture medium. Bone marrow cells (3×10^7) were injected intravenously into W/W^v mice 2 d before aortic banding. W/W^v mice with reconstituted bone marrow were killed 15 wk later. Hematocrit was measured to confirm successful reconstitution.

Morphologic and Echocardiographic Studies. After measurement of their body mass, the animals were anesthetized with ketamine (50 mg/kg) and xylazine (2.5 mg/kg). Transthoracic echocardiography was performed with a cardiac ultrasound recorder (Toshiba Power Vision), using a 7.5-MHz transducer. After the acquisition of high quality two-dimensional images, M-mode images of the left ventricle were recorded. Measurements of left ventricular enddiastolic (LVDd) and endsystolic (LVDs) internal dimensions were performed by the leading edge-to-leading edge convention adopted by the American Society of Echocardiography. Percent fractional shortening (%FS) was calculated as $\%FS = ([LVDd - LVDs]/LVDd) \times 100$.

Blood Pressure and Heart Rate Monitoring. The hemodynamic effects of aortic banding were monitored via the right carotid artery exposed through a cervical incision and isolated by blunt dissection as described by Rockman et al. (11). The lungs were dried for 120 min at 60°C and weighed again. The lung water content (LW) was calculated as LW = lung weight (wet) − lung weight (dry).

The pressure gradient across the aortic constriction was measured directly at 4 wk after operation with a 24 gauge polyethylene tube (TERUMO), inserted into the infrarenal abdominal aorta, then advanced through the stenosis to measure blood pressure at the suprarenal level. Pressure gradient was calculated as (systolic blood pressure at the suprarenal level) − (systolic blood pressure at the infrarenal level).

Histological Analysis. We examined 15 banded W/W^v mice, 14 banded WT mice, 10 sham-operated W/W^v mice, and 9 sham-operated WT mice. The hearts were fixed with 10% formalin for histological examinations. The fixed hearts were imbedded in paraffin, sectioned in 2-μm thick slices, and stained with hematoxylin-eosin for overall morphology, or with Sirius red F3BA (0.1% solution in saturated aqueous picric acid) to allow a clear discrimination between cardiac myocytes and collagen matrix (12). Changes in perivascular fibrosis were ascertained by relating the area of perivascular fibrosis to the total vessel area as described previously (13).

For transmission electron microscopy, heart specimens were fixed with Karnovsky solution (3% glutaraldehyde and 1.6% paraformaldehyde in 0.1 mol/liter phosphate buffer [PB], pH 7.4) overnight at 4°C and then were cut into 1-mm thick sections. They were postfixed in 1% osmium tetroxide in PB overnight at 4°C, dehydrated in ethanol series, and embedded in Polybed (Polysciences Inc.). 70-nm thick ultrathin sections were stained with saturated uranyl acetate and lead citrate, and observed under a JEM-1200EX electron microscope (JEOL) at 100 kV.

Measurement of Plasma Angiotensin II Level and Renin Activity. The abdomen of eight WBB6F1-W/W^v mice and seven WT mice was opened under anesthesia with ketamine and xylazine when killed at 15 wk after aortic banding. Blood was rapidly obtained by puncture of the inferior vena cava, transferred to chilled tubes containing aprotinin (1,000 kallidinogenase inactivator units per milliliter) and Na^2 EDTA (1 mg/ml), and immediately centrifuged at 4°C. Plasma samples were stored at −80°C until angiotensin II measurement by ELISA. Plasma renin activity (PRA) was determined using RENIN-RIABEAD (Dainabot).

Quantitative Reverse Transcription PCR Analysis. We examined five mice of each groups. Total RNA was isolated from the left ventricle by the acid guanidinium thiocyanate-phenol-chloroform method. Real-time quantitative PCR (TaqMan PCR) using an ABI PRISM 7700 Sequence Detection System and TaqMan PCR Core Reagent Kit (PerkinElmer) was performed according to the manufacturer's protocol. 1 μl of the first strand cDNA was used in the following assay. The following forward (F) and reverse (R) oligonucleotides, and probes (P) were used for the quantification of mouse mast cell protease (mMCP)-5, atrial natriuretic peptide (ANP), angiotensinogen and GAPDH mRNA; mMCP-5 F, 5′-TTGCCAGCCTGTGAGGAAA-3′; mMCP-5 R, 5′-TACAGACAGGCCAGATCGCAT-3′; mMCP-5 P, 5′-CTGGAACTGGAATAGTGCAGGTTTTGTGTG-3′: angiotensinogen F, 5′-TTGTCTAGGTTGGCGCTGAAG-3′; angiotensinogen R, 5′-AGATGCAGAAGATGGTGGCCT-3′; angiotensinogen P, 5′-ACACAGAAGCAAATGCACAGATCGGAGA-3′: ANP F, 5′-CCATATTGGAGCAAATCCTGTG-3′; ANP R, 5′-CTTCTACCGGCCATCTTCTCCTC-3′; ANP P, 5′-TGATGGATTTCAAGAACCTGCTAGACCACC-3′: GAPDH F, 5′-TTCACCACCATGGAGAAGGC-3′; GAPDH R, 5′-GGCATGGACTGTGGTCATGA-3′; GAPDH P, 5′-TGCATCCTGCACCACCAACTGCTTAG-3′. The conditions for the TaqMan PCR were as follows: 95°C for 10 min, followed by 40 cycles at 95°C for 15 s and 60°C for 1 min.

Apoptosis Analysis. We examined four banded W/W^v mice and five banded WT mice. Apoptotic cells were identified by terminal deoxynucleotidyl transferase UTP nick end labeling (TUNEL) assay. Hearts were harvested 15 wk after operation from banded and from sham-operated mice, fixed in 10% neutral buffered formalin, and embedded in paraffin. Paraffin section, 2-μm thick, were mounted on slides, and apoptosis was detected with an in situ Apoptosis Detection kit (Takara Shuzo Co.).

Experiment 2. These experiments were performed in 9-wk-old male C57BL/6 mice, because WT mice are semi-semisyngenic with C57BL/6 mice and the mice have been used to examine the effects of pressure overload in many previous reports. Pressure overload was produced by banding of the abdominal

aorta as described earlier. 4 wk after surgery, the animals were randomized to two groups. One group (n = 16) received tranilast, (Kissei Pharmaceutical) 100 mg/kg, orally for 11 wk. The other group (n = 20) received the vehicle for a same duration. Echocardiography was performed 4 and 15 wk after operation, and blood pressure was monitored at 15 wk as described above. Mice were killed 15 wk after the operation, and their heart and body weights were measured.

Statistical Analysis. All results are expressed as mean ± SEM. Multiple comparisons among three or more groups were performed by one-way analysis of variance (ANOVA) and Fisher's exact test for post hoc analysis. Differences were considered statistically significant at $P < 0.05$.

Results and Discussion

Experiment 1

Morphologic and Functional Effects of Pressure Overload. At 4 wk, HW/BW was significantly greater in the animals who had undergone aortic banding than in the sham-operated animals ($P < 0.05$), while no significant difference was found between the two groups of mice exposed to pressure overload (Table I). Likewise, echocardiographic left ventricular performance was preserved and comparable in both groups. No significant difference was measured between the two groups in systolic blood pressure (114.0 ± 4.1 mmHg in W/W^v mice, versus 120.1 ± 7.8 mmHg in WT mice) or in the systolic pressure gradient across the stenosis (61.0 ± 3.5 mmHg in W/W^v mice, versus 65.2 ± 11.3 mmHg in WT mice). These results suggest that mast cells play no role in compensated cardiac hypertrophy induced by pressure overload.

However, clear differences in response to pressure overload became apparent at 15 wk (Table I). Although no significant difference in systolic blood pressure was measured between the W/W^v mice (114.8 ± 7.2 mmHg) and the WT mice (106.0 ± 13.1 mmHg) who had undergone aortic banding, mean HW/BW was significantly greater in WT mice than in W/W^v mice. Table II presents the results of the echocardiographic measurements performed at baseline, and up to 15 wk after aortic banding in the W/W^v versus the WT mice. Before, and within 8 wk of the operation, there was no significant difference in left ventricular %FS, a measure of systolic function, between the two groups. Whereas mean %FS remained in the range measured preoperatively up to 15 wk after aortic banding in the W/W^v mice, it decreased significantly in the WT mice (Table II). In contrast to the WT mice, whose left ventricular dimensions increased significantly between baseline and 15 wk, the W/W^v mice had no apparent loss of systolic function (Table II). Lung weight and lung water content, corrected for body weight, were higher in WT mice than in W/W^v mice and in sham-operated mice (Table I). These observations suggest that loss of myocardial function was confined to the WT mice exposed to pressure overload. In summary, chronic pressure overload caused the deterioration of left ventricular performance, pulmonary congestion, and maladaptive hypertrophy in WT mice, while overall cardiac function remained stable in W/W^v mice. These results indicate that mast cells have a key role in the evolution from compensated to decompensated hypertrophy in pressure overloaded mice.

Histological Study. A prominent increase in perivascular fibrosis was observed only in WT mice, whereas in W/W^v mice, its extent was nearly the same as that in sham-operated mice (Fig. 1, A and B). In addition, there was a trend toward a lesser amount of interstitial fibrosis in W/W^v compared with WT mice. Likewise, TUNEL assay revealed more apoptotic cardiac myocytes in WT mice than in W/W^v mice, although the difference was not statistically significant. An attempt was made to identify apoptotic cardiac myocytes by transmission electron microscopic analysis, the confirmatory gold standard of the presence of apop-

Table I. *Morphometric and Hemodynamic Analysis*

	Preband		4 wk		15 wk	
	W/W^v	WT	W/W^v	WT	W/W^v	WT
n	5	5	9	6	12	13
BW (g)	26.3 ± 0.2	28.1 ± 0.5[a]	26.6 ± 0.4	27.9 ± 0.4[a]	30.6 ± 0.5	33.9 ± 0.5[a]
HW (mg)	114.7 ± 1.5	121.4 ± 1.5[a]	158.4 ± 11.2	171.6 ± 11.4	146.2 ± 5.4	220.5 ± 20.1[a]
Lung (wet) (mg)	139.1 ± 3.2	160.6 ± 3.2[a]	ND	ND	155.9 ± 3.6	215.4 ± 12.9[a]
LW (mg)	107.7 ± 3.0	124.1 ± 3.7[a]	ND	ND	122.7 ± 3.6	171.3 ± 14.8[a]
HW/BW (mg/g)	4.37 ± 0.07	4.32 ± 0.05	5.94 ± 0.38	6.17 ± 0.43	4.77 ± 0.12	6.53 ± 0.67[a]
Lung/BW (mg/g)	5.31 ± 0.09	5.89 ± 0.11[a]	ND	ND	5.10 ± 0.06	6.39 ± 0.66[a]
LW/BW (mg/g)	4.11 ± 0.09	4.55 ± 013[a]	ND	ND	4.1 ± 0.07	5.09 ± 0.51[a]
Syst. BP (mmHg)	ND	ND	130.4 ± 5.3	135.3 ± 10.8	114.8 ± 7.2	106.0 ± 13.1

BW, body weight; HW, heart weight; LW, lung water; Syst. BP, systolic blood pressure; ND, not done.
[a]$P < 0.05$ for W/W^v versus WT.

Table II. *Echocardiographic Measures in Preband and Postband Mice*

	Preband		8 wk		11 wk		15 wk	
	W/W^v	WT	W/W^v	WT	W/W^v	WT	W/W^v	WT
LVDd (mm)	2.96 ± 0.12	2.86 ± 0.09	3.08 ± 0.17	3.40 ± 0.14	3.12 ± 0.11	3.52 ± 0.10	3.02 ± 0.17	3.60 ± 0.19[a]
LVDs (mm)	0.80 ± 0.04	0.80 ± 0.03	0.73 ± 0.11	0.99 ± 0.09	0.89 ± 0.08	1.35 ± 0.17[a]	0.77 ± 0.08	1.85 ± 0.27[a]
%FS	72.8 ± 1.8	71.9 ± 1.5	77.2 ± 2.5	71.2 ± 1.9	71.6 ± 2.0	62.2 ± 4.1[a]	75.1 ± 1.8	50.6 ± 4.8[a]

LVDd, end-diastolic left ventricular internal dimension; LVDs, end-systolic left ventricular internal dimension; %FS, left ventricular percent fractional shortening.
[a]$P < 0.05$ for W/W^v versus WT.

tosis. However, no apoptotic myocytes were found, probably because of their low density in our experimental model. However, a decrease in myofilamments, mitochondrial degeneration, and accumulation of lipid droplets were observed in WT mice (Fig. 1 C). These were rarely found in W/W^v mice.

The number of mast cells, at 15 wk, was significantly greater in the hearts of banded (12.2 ± 1.7 mast cells/slice) than of sham-operated (5.5 ± 1.3 mast cells/slice) WT mice ($P = 0.0001$). Mast cells were not detectable in W/W^v mice.

Expression of Chymase Gene. As we had previously hypothesized that mast cell chymase plays a role in the pathophysiology of heart failure (7), we examined the upregulation of mMCP-5, the counterpart of human chymase. The evolution of the relative levels of mMCP-5 is shown in Fig. 2 A. The gene expression levels of mMCP-5 after aortic banding were significantly higher in WT mice than in W/W^v mice.

Effects of Angiotensin II. No significant difference was found in mean plasma angiotensin II level between W/W^v mice (217.3 ± 66.7 pg/ml) and WT mice (249.1 ± 63.7 pg/ml) exposed to pressure overload (Fig. 2 B). Likewise, the gene expression levels of angiotensinogen in the hearts were comparable among all study groups (Fig. 2 C). Plasma renin activity (PRA) in mast cell deficient W/W^v mice (9-wk-old, $n = 3$) or WT mice (9-wk-old, $n = 3$) was also measured. PRA was 1.0 ± 0.47 ng/ml/h in W/W^v mice, versus 0.89 ± 0.43 ng/ml/h in WT mice, a nonsignificant difference.

Effects of Chronic Pressure Overload on Fetal Gene Expression. We had verified that, in our experimental models, mRNA levels of ANP were increased 4 wk after aortic banding (data not shown). At 15 wk after operation, ANP mRNA levels were increased in banded mice, and they were higher in WT mice than in W/W^v mice (Fig. 2 D).

Reconstitution of Mast Cells and Bone Marrow Cells. Cardiac mast cells were not reconstituted by the transfusion of bone marrow–derived mast cells or bone marrow cells, although mast cells were reconstituted in other murine tissues, such as lungs. Consequently, we could not verify the

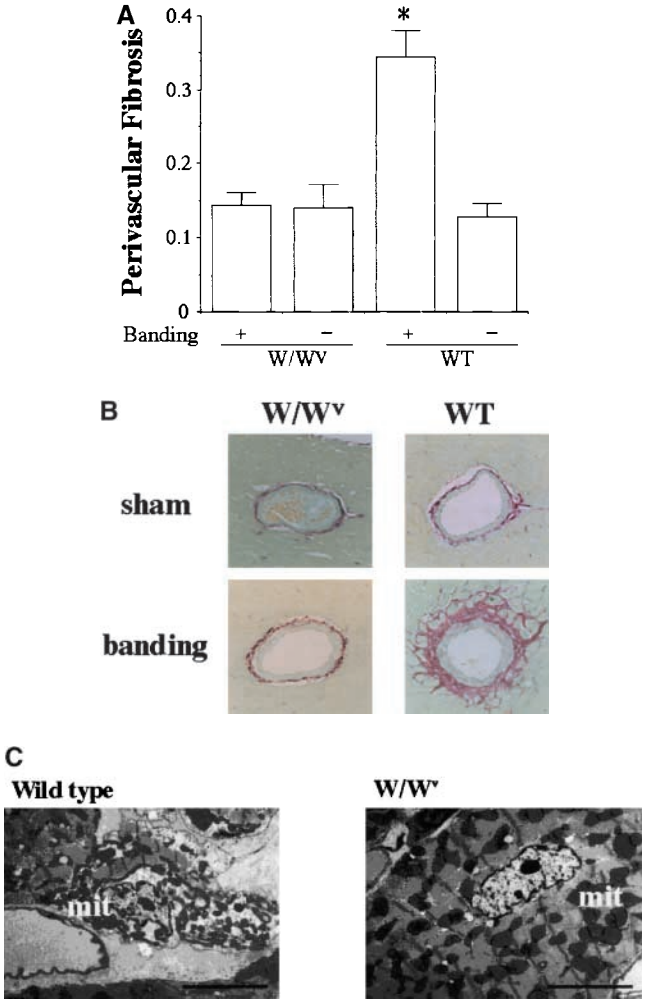

Figure 1. Microscopic analysis at 15 wk after aortic banding. (A) Relative area of fibrosis. Values are mean ± SEM. *$P < 0.05$ vs. W/W^v mice and sham operated mice. (B) Histological staining of left ventricular fibrosis (Sirius red). Perivascular collagen accumulation (red) is more prominent in WT hypertensive mouse. Original magnification, ×200. +, banded mice; −, sham-operated mice. (C) Transmission electron microscopy. In WT mice (left panel), clusters of mitochondria (mit) of various shape and size were noted. A decrease in the density of myofibrils is also apparent. Original magnification, ×5,000. Bar, 5 μm.

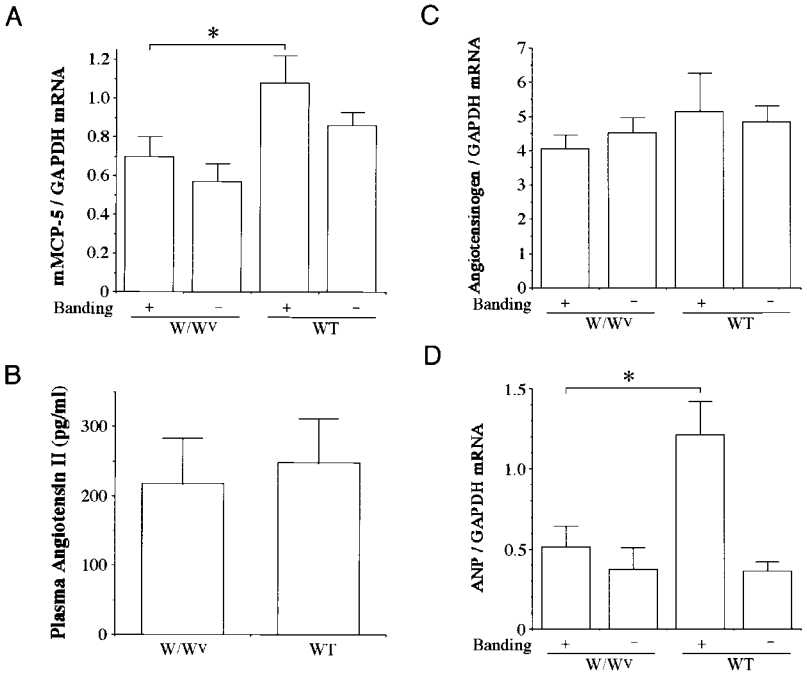

Figure 2. Real-time quantitative PCR analysis and angiotensin II concentrations in plasma. (A) mRNA levels of mMCP-5. (B) Angiotensin II concentrations in plasma. (C) mRNA levels of angiotensinogen in the hearts. (D) mRNA levels of ANP. +, banded mice; −, sham-operated mice. Values represent the normalized mean ± SEM. $^*P < 0.05$.

roles played by mast cells by their reconstitution. Reconstitution of bone marrow cells mitigated the anemia; hematocrit was 28 ± 2.6% in W/W^v mice (24-wk-old, $n = 4$), versus 34 ± 0.9% in W/W^v mice (24-wk-old, $n = 5$) with reconstituted bone marrow cells. However, maladaptive cardiac hypertrophy or decreased cardiac systolic function were observed neither in W/W^v mice nor in W/W^v mice with reconstituted bone marrow cells. This suggests that anemia was not the reason for the absence of heart failure progression in W/W^v mice.

Experiment 2

Effects of Tranilast on Cardiac Dimensions and Function. The mutation of W/c-kit produces receptors with markedly deficient tyrosine kinase activity, resulting not only in mast cell deficiency but also in anemia, lack of melanocytes in the skin, and sterility (14). The degree of anemia in mast cell deficient W/W^v mice (9-wk-old, $n = 3$) or WT mice (9-wk-old, $n = 3$), unexposed to pressure overload, was examined. Hematocrit was 37.9 ± 1.3% in W/W^v mice, versus 53.3 ± 1.2% in WT mice, and hemoglobin concentration was 10.2 ± 0.8 g/dl in W/W^v mice, versus 14.6 ± 0.3 g/dl in WT mice. To further examine the role of mast cells in the progression of heart failure, the effects of tranilast, a mast cell stabilizer, were studied in 9-wk-old male C57BL/6 mice. Baseline echocardiograms confirmed comparable left ventricular dimensions and systolic function in the tranilast- versus the vehicle-treated groups. At 15 wk after aortic banding, no significant difference was measured in systolic blood pressure between the tranilast-treated and the control groups (Fig. 3 A). However, treatment with tranilast significantly limited the development of cardiac hypertrophy (Fig. 3 B), fall in %FS (Fig. 3 C), and left ventricular chamber dilatation (Fig. 3 D). Combined with the results of experiment 1, these observations suggest that mast cells amplify the pathophysiologic manifestations of heart failure in pressure-overloaded mice.

This study showed that a mutation at the W/c-kit locus, and treatment with tranilast prevented the evolution from compensated hypertrophy to heart failure in a murine

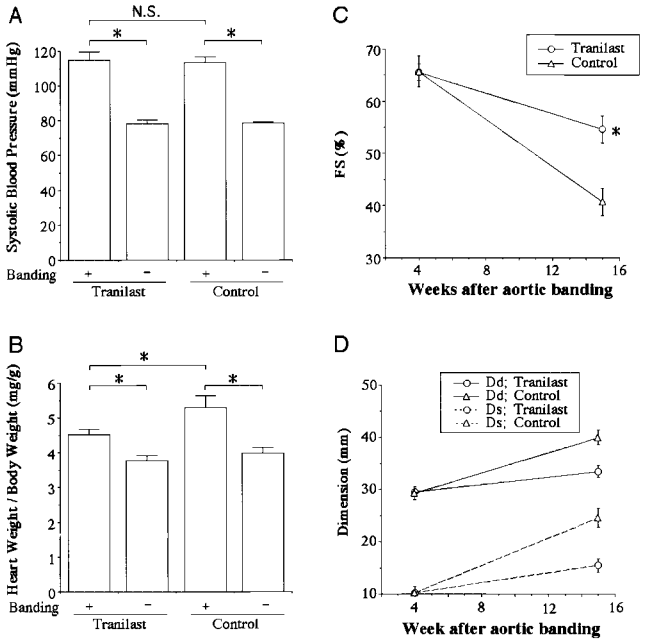

Figure 3. Effects of tranilast on blood pressure, heart weight and echocardiographic measurements. (A) Arterial blood pressure. (B) Heart weight (mg)/body weight (g) ratio. (C) Left ventricular percent fractional shortening (FS). (D) Left ventricular dimensions. Dd, enddiastolic diameter; Ds, endsystolic diameter. Values are mean ± SEM. $^*P < 0.05$. +, banded mice; −, sham-operated mice.

model of systolic pressure overload. This is the first in vivo demonstration of a direct contribution of W/c-kit in the pathogenesis of heart failure, and our results strongly implicate mast cells in this process.

Our experiments showed that mast cell deficiency attenuated the development of myocardial fibrosis and systolic pressure overload-induced hypertrophy. As each of these processes is likely to cause cardiac dysfunction, the mechanisms by which mast cells promote heart failure should be discussed in light of them. First, myocardial fibrosis induced by mast cells may impair diastolic function. In this study, perivascular fibrosis was prominent in WT mice, but not in W/W^v mice. This indicates that mast cells play a role in the development of myocardial fibrosis found in pressure-overloaded hearts. It has been reported that the number of mast cells is increased in fibrotic diseases of skin (15) and lung. Mast cells have also been found to induce proliferation of fibroblasts by various mediators in vitro, such as chymase (7), histamine, and tryptase (16). Patella et al. have recently described an increase in mast cells in the hearts of dilated and ischemic cardiomyopathy (6), where fibrosis is prominent. Consequently, it appears very likely that mast cells induce myocardial fibrosis as part of the development of heart failure. Second, mast cells may promote cardiac maladaptive hypertrophy. At 15 wk, the W/W^v mice had mild concentric left ventricular hypertrophy with preserved systolic function. In contrast, marked cardiac hypertrophy and ventricular dilatation with reduced %FS were observed in the WT mice, suggesting that mast cells promote maladaptive hypertrophy, ventricular dilatation, and cardiac decompensation. These cardiac changes may be caused by bioactive peptides such as angiotensin II and endothelin 1, also known to induce hypertrophy of cardiac myocytes and myocardial fibrosis. However, the involvement of angiotensin II was not clarified in our study. Endothelin 1 is another potent mediator, which can induce hypertrophy of cardiac myocytes and proliferation of cardiac fibroblasts. Mast cell chymase is reported to activate big endothelin to endothelin 1 (17). We have previously reported that mast cell chymase induces apoptosis of cardiac myocytes in vitro (7). In addition, chymase has been implicated in tissue remodeling through activation of matrix metalloproteinases (18) and IL-1β precursors (19), and proliferation of fibroblasts (7). These observations suggest that the modulation of tissue remodeling by chymase was one of the mechanisms of heart failure progression in our study.

Other mediators contained in mast cell granules, such as tryptase and cytokines, might play a role in cardiac changes caused by systolic pressure overload (20). We do not exclude the possibility that maladaptive hypertrophy was partly induced by a direct interaction between stem cell factor and c-kit. The undefined role of stem cell factor in cardiovascular diseases is in need of further research.

The number of mast cells and mMCP-5 mRNA level, major mediator of mast cells, were significantly greater in banded WT mice than in sham-operated mice. This suggests that mast cells are upregulated in pressure overloaded mice.

Tranilast, N-(3,4-dimethoxycinnamoyl) anthranillic acid, is an oral antiallergic drug used in Japan. Its antiallergic effects are mainly mediated by the inhibition of the release of chemical mediators from mast cells. It has been described as effective in the prevention of coronary restenosis after directional coronary atherectomy in humans (21), and in the suppression of neointima formation in balloon-injured dog carotid artery (22). Furthermore, tranilast suppresses the vascular expression of chymase (22). Therefore, we hypothesize that the effects of tranilast in the prevention of heart failure in our study were mainly due to the suppression of mast cell degranulation and inhibition of mast cell chymase.

In conclusion, we present several lines of evidence indicating that mast cells play a role in the evolution from compensated hypertrophy to congestive heart failure. As mast cell stabilizers, including tranilast, are safely used as antiallergic agents in Japan, we are planning to examine whether they may be a new option in the management of heart failure.

We thank Ms. Shoko Sakai and Ms. Yoko Okazaki for their technical assistance.

This work was supported in part by a Research Grant from the Japanese Ministry of Health and Welfare and a Grant for Scientific Research from the Japanese Ministry of Education, Science and Culture.

Submitted: 7 December 2000
Revised: 24 December 2000
Accepted: 18 December 2001

References

1. Diez, J., M.A. Fortuno, and S. Ravassa. 1998. Apoptosis in hypertensive heart disease. *Curr. Opin. Cardiol.* 13:317–325.
2. Matsumori, A. 1997. Molecular and immune mechanisms in the pathogenesis of cardiomyopathy—role of viruses, cytokines, and nitric oxide. *Jpn. Circ. J.* 61:275–291.
3. Dvorak, A.M. 1986. Mast-cell degranulation in human hearts. *N. Engl. J. Med.* 315:969–970.
4. Marone, G., G. de-Crescenzo, M. Adt, V. Patella, E. Arbustini, and A. Genovese. 1995. Immunological characterization and functional importance of human heart mast cells. *Immunopharmacology.* 31:1–18.
5. Panizo, A., F.J. Mindan, M.F. Galindo, E. Cenarruzabeitia, M. Hernandez, and J. Diez. 1995. Are mast cells involved in hypertensive heart disease? *J. Hypertens.* 13:1201–1208.
6. Patella, V., I. Marino, E. Arbustini, B. Lampater-Schummert, L. Verga, M. Adt, and G. Marone. 1998. Stem cell factor in mast cells and increased mast cell density in idiopathic and ischemic cardiomyopathy. *Circulation.* 97:971–978.
7. Hara, M., A. Matsumori, K. Ono, H. Kido, M. Hwang, T. Miyamoto, A. Iwasaki, M. Okada, K. Nakatani, and S. Sasayama. 1999. Mast cells cause apoptosis of cardiomyocytes and proliferation of other intramyocardial cells in vitro. *Circulation.* 100:1443–1449.
8. Harada, K., I. Komuro, I. Shiojima, D. Hayashi, S. Kudoh, T. Mizuno, K. Kijima, H. Matsubara, T. Sugaya, K. Murakami, and Y. Yazaki. 1998. Pressure overload induces cardiac hypertrophy in angiotensin II type 1A receptor knockout mice. *Circulation.* 97:1952–1959.

9. Malaviya, R., T. Ikeda, E. Ross, and S.N. Abraham. 1996. Mast cell modulation of neutrophil influx and bacterial clearance at sites of infection through TNF-alpha. *Nature.* 381:77–80.
10. Wang, L., A. Stanisz, B. Wershil, S. Galli, and M. Perdue. 1995. Substance P induces ion secretion in mouse small intestine through effects of enteric nerves and mast cells. *Am. J. Physiol.* 269:G85–G92.
11. Rockman, H.A., S.P. Wachhorst, L. Mao, and J. Ross, Jr. 1994. ANG II receptor blockade prevents ventricular hypertrophy and ANF gene expression with pressure overload in mice. *Am. J. Physiol.* 266:H2468–H2475.
12. Ono, K., A. Matsumori, T. Shioi, Y. Furukawa, and S. Sasayama. 1998. Cytokine gene expression after myocardial infarction in rat hearts: possible implication in left ventricular remodeling. *Circulation.* 98:149–156.
13. Nicoletti, A., D. Heudes, N. Hinglais, M.D. Appay, M. Philippe, C. Sassy-Prigent, J. Bariety, and J.B. Michel. 1995. Left ventricular fibrosis in renovascular hypertensive rats. Effect of losartan and spironolactone. *Hypertension.* 26:101–111.
14. Nocka, K. 1990. Molecular bases of dominant negative and loss of function mutations at the murine c-kit/white spotting locus. *EMBO J.* 9:1805–1813.
15. Nishioka, K., Y. Kobayashi, I. Katayama, and C. Takijiri. 1987. Mast cell numbers in diffuse scleroderma. *Arch. Dermatol.* 123:205–208.
16. Ruoss, S.J., T. Hartmann, and G.H. Caughey. 1991. Mast cell tryptase is a mitogen for cultured fibroblasts. *J. Clin. Invest.* 88:493–499.
17. Marone, G., G. de-Crescenzo, V. Patella, and A. Genovese. 1998. Human cardiac mast cells and their role in severe allergic reaction. *In* Asthma and Allergic Diseases. Academic Press Ltd., London. 237–269.
18. Lees, M., D.J. Taylor, and D.E. Woolley. 1994. Mast cell proteinases activate precursor forms of collagenase and stromelysin, but not of gelatinases A and B. *Eur. J. Biochem.* 223:171–177.
19. Mizutani, H., N. Schechter, G. Lazarus, R.A. Black, and T.S. Kupper. 1991. Rapid and specific conversion of precursor interleukin 1 beta (IL-1 beta) to an active IL-1 species by human mast cell chymase. *J. Exp. Med.* 174:821–825.
20. Galli, S.J., and B.K. Wershil. 1995. Mouse mast cell cytokine production: role in cutaneous inflammatory and immunological responses. *Exp. Dermatol.* 4:240–249.
21. Kosuga, K., H. Tamai, K. Ueda, Y.S. Hsu, S. Ono, S. Tanaka, T. Doi, W. Myou-U, S. Motohara, and H. Uehata. 1997. Effectiveness of tranilast on restenosis after directional coronary atherectomy. *Am. Heart J.* 134:712–718.
22. Shiota, N., H. Okunishi, S. Takai, I. Mikoshiba, H. Sakonjo, N. Shibata, and M. Miyazaki. 1999. Tranilast suppresses vascular chymase expression and neointima formation in balloon-injured dog carotid artery. *Circulation.* 99:1084–1090.